Rise of calcispheres during the Carnian Pluvial Episode (Late Triassic)

Jacopo Dal Corso, Nereo Preto, Claudia Agnini, Sönke Hohn, Agostino Merico, Helmut Willems, Piero Gianolla

PII: S0921-8181(21)00038-2

DOI: https://doi.org/10.1016/j.gloplacha.2021.103453

Reference: GLOBAL 103453

To appear in: *Global and Planetary Change*

Received date: 31 December 2019

Revised date: 13 January 2021

Accepted date: 4 February 2021

Please cite this article as: J.D. Corso, N. Preto, C. Agnini, et al., Rise of calcispheres during the Carnian Pluvial Episode (Late Triassic), *Global and Planetary Change* (2019), https://doi.org/10.1016/j.gloplacha.2021.103453

Rise of calcispheres during the Carnian Pluvial Episode (Late Triassic)

Jacopo Dal Corso[1*], j.dalcorso@cug.edu.cn,Nereo Preto[2],Claudia Agnini[2],Sönke Hohn[3],Agostino Merico[3,4],Helmut Willems[5],Piero Gianolla[6]

[1]State Key Laboratory of Biogeology and Environmental Geology, School of Earth Sciences, China University of Geosciences, Wuhan, China.

[2]Dipartimento di Geoscienze, University of Padua, Padova, Italy.

[3]Leibniz Centre for Tropical Marine Research, Bremen, Germany.

[4]Department of Physics and Earth Sciences, Jacobs University Bremen, Bremen, Germany

[5]Department of Earth Sciences, University of Bremen, Bremen, Germany.

[6]Dipartimento di Fisica e Scienze della Terra , University of Ferrara, Ferrara, Italy.

[*]corresponding author

ABSTRACT

It has been argued that the beginning of significant pelagic calcification could have been linked to the Carnian Pluvial Episode (CPE), a climate change in the Late Triassic (~234–232 Ma) that was marked by C-cycle disruption and global warming. Nevertheless, abundant calcareous nannofossils have been described so far only in post-CPE rocks, and therefore no conclusive hypotheses can be drawn on possible causal links with it. Here we show that in deep-water successions of the Western Tethys, *Orthopithonella* calcispheres interpreted as calcareous dinocysts became an important component of carbonate sedimentation from the onset of the CPE, and could constitute up to 8% of hemipelagic limestones. Before the CPE, in similar depositional environments, calcispheres are rare or absent, and never constitute a significant part of the sediment. This change in the deep-water carbonate sedimentation, is mirrored in the shallow water environments by the rise of the reefs built by Scleractinia corals. These important innovations in Earth's carbonate systems may indicate a deep

modification in the ocean biogeochemistry during the CPE.

Keywords: Triassic, Carnian Pluvial Episode, calcispheres, pelagic biocalcification

1. Introduction

Pelagic biocalcification became significant from the Early Jurassic with the diversification and speciation of coccolithophores (e.g., Bown et al., 2004; Erba, 2006; Suchéras-Marx et al., 2019), but calcifying nannofossils appeared and were episodically abundant already during the Triassic (e.g., Bown, 1992; Bown et al., 2004; Falkowski 2004; Erba, 2006; Gardin et al., 2012; Preto et al., 2013a, b; Demangel et al., 2020). Pre-Triassic calcareous nannofossils in Silurian, Carboniferous, and Permian rocks are of uncertain affinity, very rare, and observed only locally (e.g., Bown et al., 2004; Munnecke and Servais, 2008).

Abundant calcispheres are found in Carnian successions (e.g., Jafar, 1983; Janofske, 1992; Bown et al., 2004; Onoue and Yoshida, 2010; Preto et al., 2013a; Dal Corso et al., 2020). Late Triassic calcispheres are *Obliquipithonella*, *Orthopithonella*, and *Prinsiosphaera* (Jafar, 1983; Janofske, 1992; Bown et al., 2004; Onoue and Yoshida, 2010), and it has been pointed out that the oldest Carnian calcispheres, and in particular *Orthopithonella*, may have had planktonic calcareous dinoflagellate affinity (Janofske, 1992; Preto et al., 2013a). Janofske (1992) reported the presence of these calcareous dinocysts (*Orthopithonella* and *Obliquipithonella*) from the Carnian (Misurina section) of the Dolomites (Southern Alps, Italy). Onoue and Yoshida (2010) found similar calcispheres in the Late Carnian – Middle Norian deep, open ocean successions of Japan. Preto et al. (2013a, b) showed that in Late Carnian and Norian hemipelagic periplatform deposits of the Lagonegro and Sicanian basins in southern Italy, calcispheres are abundant, but are instead very rare in the Early Carnian. Overall, these works suggest that pelagic carbonate bioproduction occurred in the Late Carnian (Tuvalian) (Onoue and Yoshida, 2010; Preto et al., 2013). Furin et al. (2006) and Preto et al. (2013a) also pointed out that this important event happened just after a major climate change known as the Carnian Pluvial Episode

(CPE), proposing a possible link between the evolution of this group and climate change.

The onset of the CPE is marked by a sharp 2–4‰ negative C-isotope excursion (NCIE) recorded by bulk organic matter and biomarkers (Dal Corso et al., 2012, 2015; Mueller et al., 2016a, b). Further NCIEs follow the first one, as recorded by organic and carbonate C-isotope records from stratigraphic successions of the Southern Alps, Hungary, UK, Oman, China and Japan (Sun et al., 2016, 2019; Miller et al., 2017; Dal Corso et al., 2018a, 2020; Tomimatsu et al., 2021). In western Tethys each NCIE just precede thick piles of siliciclastic rocks in the sedimentary records, within widespread generally more humid conditions during the CPE (Dal Corso et al., 2018a, b, 2019). This suggests multiple injections of ^{13}C-depleted carbon into the Carnian atmosphere–ocean system that repeatedly enhanced the hydrological cycle, leading to the massive transport of siliciclastic material into the basins (Dal Corso et al., 2018a). At the CPE, a sudden reduction of carbonate precipitation in shallow water environments of western Tethys is also observed (Schlager and Schöllnberger, 1974; Simms and Ruffell, 1989; Preto and Hinnov, 2003; Keim et al., 2006; Hornung et al., 2007; Stefani et al., 2010), and is accompanied by a Tethys-wide switch from microbial to metazoan factories (Gattolin et al., 2015; Dal Corso et al., 2015, 2018a, 2020, Jin et al., 2020).

Preto et al. (2013a) proposed that the rise of calcispheres, which they observed after the CPE, could have been triggered by increasing seawater alkalinity and supersaturation due to enhanced supply of bicarbonate from rivers, coupled to reduced shallow-water carbonate precipitation. The work of Preto et al. (2013) however, had two main limitations: (1) due to the strong overgrowth of diagenetic calcite around calcispheres, a precise evaluation of the proportion of pelagic carbonate to the total sediment budget could not be achieved; (2) the causal link between the CPE and the spread of calcispheres was weak, since carbonates (including the calcispheres) are not preserved around the CPE in the deep Lagonegro Basin because of a rise of the carbonate compensation depth, CCD (Rigo et al., 2007).

In this study, we investigated the occurrence and abundance of calcispheres, of possible

dinoflagellate affinity, in shales and limestones from well-calibrated Carnian deep-water successions in various localities of western Tethys across the CPE. We show that these calcispheres rose during the CPE and were widespread throughout the western Tethys at least.

2. Geological setting and studied sections

2.1 Transdanubian Range, Hungary

Samples come from outcrops and core material (Balatonfüred borehole, Bfü-1) from the Transdanubian Range in Hungary (Fig. 1). The stratigraphic succession of the Transdanubian Range considered for this study encompasses the entire Julian (Early Carnian; Dal Corso et al., 2015 and references therein). It starts with the pelagic cherty nodular limestones of the Füred Formation, which overlies the upper Ladinian Buchenstein Formation. The Füred Fm. is relatively poor in fossils. Early Carnian ammonoids (*Trachyceras* zone: *Trachyceras aon*, *Frankites* sp., *Sirenites* sp.), bivalves, brachiopods and conodonts (*Gladigondollela tethydis*, *Paragondolella foliata*, *Paragondolella foliata inclinata*, etc.) were occasionally found (Dal Corso et al., 2015, 2018a; Fig. 2). *Neoprotrachyceras* spp. and *Sirenites* sp. of the *Austrotrachyceras* ammonoid zone were found in the clay-rich uppermost part of the Füred Fm. (Budai et al., 1999; Krystyn, 1978; Lukeneder and Lukeneder, 2013). Therefore, the base of the *Austrotrachyceras* ammonoid zone is placed in the uppermost part of the Füred Fm. (Dal Corso et al., 2015; Fig. 2). An abrupt increase in the fine siliciclastic fraction marks the transition to the Mencshely Member of the Veszprém Fm., and consists of dark-grey thin-bedded laminated and bioturbated marls with silt–sand intercalations and increasing kaolinite content, which testify to increasing humid conditions related to the onset of the CPE (Rostási et al., 2011). The NCIE, that marks the onset of the CPE, starts in the uppermost part of the Füred Fm.–lowermost part of the Veszprém Fm. (Dal Corso et al., 2015; Fig. 3). Within the Mencshely Member (Veszprém Fm.), a second NCIE is recorded by total organic carbon isotopes (Dal Corso et al., 2018a; Fig. 3). The Mencshely Member passes abruptly to a 10–12 m thick package of well bedded micritic limestone ascribable to the Nosztor Limestone Member

(Veszprém Fm.), whose age is constrained by the presence of ammonoids defining the *Austrotrachyceras* ammonoid zone (Budai et al., 1999; Fig. 2). The Nosztor Limestone Member is overlain by grey to dark grey marls and clays of the Csicsó Member (Veszprém Fm.), lithologically very similar to, and almost indistinguishable from the Mencshely Member (Budai et al., 1999). *Neoprotrachyceras baconicum* was found in the Csicsó Member (Budai et al., 1999), which still correlate with the *Austrotrachyceras* ammonoid zone. Sporomorphs of the *Aulisporites astigmosus* assemblage (*sensu* Roghi et al., 2010) are present throughout the all Veszprém Fm. (Baranyi et al., 2019), confirming a Julian 2 age for this formation (Fig. 1 and 2). The Veszprém Fm. is overlain by the shallow-water carbonates of the Sándorhegy Fm. For this study, we studied eight selected lime mudstone samples from both outcrops (Csukrét Section; see Góczán et al., 1991) and a borehole (BFÜ-1; Table 1), and fifty-three shale samples from boreholes (BFÜ-1 and MET-1; see Rostási et al., 2011 and Dal Corso et al., 2015, 2018a for details). This is because along the Csukrét river the shales of the Veszprém Fm. do not outcrop well and large parts of the section is covered, whilst the boreholes provide a continuous record of the succession at the base of the Veszprém Fm. (Mencshely Member) but do not encompass the Nosztor Limestone Member. Lime mudstones with radiolarian moulds and thin-shelled bivalves sampled from the Füred Fm., from the Mencshely Member (Veszprém Fm.) and from the Nosztor Limestone Member of the Veszprém Fm., were analysed in thin section and at the Field Emission Scanning Electron Microscope (FESEM). Samples from the shales of the Mencshely Member of the Veszprém Fm. were prepared as standard smear slides (Bown and Young, 1998) and observed at 1250 magnification under a polarizing microscope at the Department of Geosciences, University of Padova.

2.2 Eastern Julian Alps, Slovenia

Five samples from the eastern Julian Alps (Fig. 1) were analysed at FESEM from the lower member of the Martuljek platy limestone at the Mt. Škrlatica section (Celarc and Kolar-Jurkovšek, 2008; Celarc et

al., 2014; Jin et al., 2020). The lithostratigraphic unit can be subdivided in two members. The lower one consists in thin bedded (wavy to planar bedding) red and grey pelagic limestone (wackstone, packstone with glauconite and thin-shelled bivalves) resting, with a sharp contact, above the shallow water Rostor Limestone (Celarc and Kolar-Jurkovšek, 2008). The upper member consists of light grey to white platy limestone (packstones and grainstones), often dolomitized, characterized by un upward increase of platform derived detritus, upward the Martuljek platy limestone is bound by clinostratified grainstones, rudstones and breccias of the toe of slope facies of the Dachstein carbonate platform. The age of the Martuljek platy limestone is constrained to the late Carnian – early Norian by ammonoid and conodont biostratigraphies, the age of the lower member is constrained to the Tuvalian 2 and Tuvalian 3 (Celarc and Kolar-Jurkovšek, 2008; Celarc et al., 2014; Gale et al., 2015; Fig. 2).

2.2.1 Western Julian Alps, Italy

One (pre-CPE) lime mudstone sample from the Predil Limestone Fm. (Julian 1) and two (end of the CPE) lime mudstone samples from the western Julian Alps (Eastern Southern Alps) (Fig. 1) were analysed at FESEM from the Carnitza Fm. at Portella Pass near Cave del Predil. The Carnitza Fm. formation consists in well layered lime mudstone to wackestone with chert nodules, radiolarian moulds and abundant thin-shelled bivalves, and, occasionally, ammonoids. It is the deep-water counterpart of the Dolomia Principale epicontinental carbonate platform during the Late Carnian (Gianolla et al., 2003; Caggiati et al., 2018). The age of the Carnitza Fm. is constrained to the Tuvalian 2 – Tuvalian 3 by ammonoid, conodont and sporomorph biostratigraphies (De Zanche et al., 2000; Gianolla et al., 2003; Roghi et al., 2010; Dal Corso et al., 2018a; Fig. 2).

2.4 Dolomites, Southern Alps, Italy

Fifteen samples from the Dolomites come from the Borca Member of the Heiligkreuz Fm. (Milieres section: Dal Corso et al., 2012; Fig. 1). The Milieres section deposited in an offshore/prodelta

sedimentary environment, and consists of silty shales and marls, with cm-thick intercalations of lime mudstones, packstones and grainstones. The age of Milieres section is constrained by sporomorph, ammonoid and conodont biostratigraphies. The base of Julian 2 biochronozone is placed at the boundary between the *Concentricisporites bianulatus* and *Aulisporites astigmosus* sporomorph assemblages (Dal Corso et al., 2012; 2018; Fig. 2). Moreover, conodonts of Julian 1 age have been extracted from the lowermost Heligkreuz Fm. in other localities (Mastandrea, 1994). The first NCIE of the CPE has been found at Milieres, and it is recorded by the carbon isotopes measured on the total organic matter, higher plant n-alkanes and other marine algal biomarkers (Dal Corso et al., 2012). In addition to the samples from Milieres section covering the CPE, we analysed selected Late Permian to Late Triassic (Early Carnian) samples of deep water, fine grained carbonates from previous fieldwork in the Dolomites to check for the presence of calcispheres. These samples come from the Werfen Fm. and Bellerophon Fm. (Late Permian – Early Triassic), the Dont Fm. and Gracilis Fm. (Pelsonian, Anisian), the Morbiac Fm. (Illirian, Anisian), the Bivera, Ambata and Livinallongo Fms. (Illirian – Fassanian, Anisian – Ladinian), the Aquatona, Fernazza and Wengen Fm. (Longobardian, Ladinian) and the San Cassian Fm. (early Carnian) (for a general stratigraphic framework of the pre-CPE succession of the Dolomites please refer to e.g., Stefani et al., 2010).

3. Methods

3.1. Analysis of lime mudstone samples at FESEM

Lime mudstones were analysed at the Field Emission Scanning Electron Microscope (FESEM). Samples were cut in ~5×5 mm cubes. The cubes were attached to a microscope glass with the surface perpendicular to bedding exposed, and were etched for 20–30 seconds in 0.3% HCl to highlight crystal boundaries (Preto et al., 2013a), then cleaned in an ultrasonic bath and rinsed with deionized water. Before analysis at the FESEM the samples were coated with gold. SEM images were taken with the Zeiss SUPRA 40 of the Department of Geosciences, University of Bremen. Eighty-six pre-CPE Late

Permian to Late Triassic (Early Carnian) samples of deep water, fine grained carbonates from the Dolomites were analysed to exclude that the calcispheres were ever common before the CPE. These add to 32 Middle Triassic samples of the Dolomites from Preto et al. (2009), which were further prepared for observation under the FESEM in the context of this work. 16 syn-CPE fine carbonate, deep water samples from the Transdanubian Range, Eastern and Western Julian Alps were analysed more in detail. Samples from the (pre-CPE) deep water, fine grained Füred limestone of Hungary were also observed at the SEM to confirm that calcispheres were rare or absent before the CPE. The calcisphere carbonate production was estimated by counting 500 points on 5–8 FESEM images (see Fig. A1 in the Appendices) per sample, corresponding to an area of ca. 400x400 μm, with 2500-4000 points counted per sample. For point counting, we placed each count into one of the following main groups of limestone elements: micrite (microsparite), calcisphere, syntaxial calcite overgrowth on calcispheres, other skeletal grains, and non-carbonate elements. Points were attributed to the category "calcisphere" both when they corresponded to the test of a complete calcisphere, or to a fragment (a very rare case), because the intent of point counting was to estimate the volume proportion of carbonate derived from calcisphere, and not the number of individuals. Since the point counting has been made on SEM images, no correction is needed for the overestimation that typically affects point counting of small objects in thin section (Chayes, 1956). More details on this method are given in Preto et al. (2013b).

3.1. Smear slides analysis of shale samples under transmitted light microscope

46 samples of shale from the (syn-CPE) Mencshely Member of the Veszprém Fm. in the Transdanubian Range (Fig. 1) have been selected for the examination of the calcareous nannofossil content under transmitted light microscope (Fig. A2 in the Appendices). Smear slides were prepared using a standard procedure (Bown and Young, 1998). A qualitative estimation of the abundance of dinocysts was recorded based on the number of fragments of calcispheres per field of view (FOV), as

follows: A = abundant (>10–100 specimens per field of view); C = common (>1–10 specimens per field of view); S = scarce (1 specimen per 1–10 fields of view); R = rare (<1 specimen per 10 fields of view), VR = very rare (<5 specimens seen while logging slide). Where present calcispheres display a moderate to good preservation and the presence of whole specimens of dinocysts confirm the good state of preservation.

4. Results

The calcispheres and their occurrences in lime mudstones and shales from the studied successions are shown in Figs. 2–4. Large-field images of selected samples studied at the FESEM (limestone) and light microscope (shale) are shown in the appendices (Fig. A1 and A2). FESEM point counting data are given in the appendices (Table A1). Abundances of the calcispheres in limestone are shown in Table 1 and Fig. 3. A qualitative estimate of calcispheres' abundance in shale samples is presented in Fig. 3.

4.1 FESEM analysis

4.1.2 Transdanubian Range, Hungary

Lime mudstone samples from the Nosztor Limestone Member (Veszprém Fm.) of Hungary contain calcispheres that can be compared to those found in late Carnian to Norian carbonate deposits by Janofske (1992), Bellanca et al. (1995) and Preto et al. (2012; 2013a). No calcispheres have been found in the samples from the older Menchley Marls (Veszprém Fm.) and Füred Fm. (Fig. 2). The calcispheres of the Nosztor Limestone are better preserved than many of these previous studies, with the exception of Jafar (1983) and Janofske (1992), because overgrowths of diagenetic calcite are minimal or absent (Fig. 4G, H). A few calcispheres from the Nosztor Limestone Member do have a diagenetic overgrowth, made of elongated calcite crystals disposed radially around the calcisphere test (Fig. 4B, D). This calcite overgrowth is the most commonly observed diagenetic alteration of these Triassic calcispheres (e.g., Bellanca et al., 1995; Preto et al., 2013a; see also Fig. 4F). In some samples

of the Nosztor Limestone Member, however, calcispheres are not affected by this diagenetic modification, and the description of their test is based on these best-preserved samples. Calcispheres from the Nosztor Limestone Member are hollow spheres with a diameter of 10 μm on average, and have a test 1 to 1.5 μm thick made of sub-micrometric calcite crystals (based on 16 calcispheres sectioned at a great circle). The shape of crystals is not regular, but they are not elongated radially and often appear as rhombohedra with the c-axis roughly disposed radially (Fig. 4). The test is made of at least two layers of such rhombohedral or sub-rhomboedral crystals, and in best preserved specimens (e.g., Fig. 4G, H), the calcite crystals of the surrounding cement and microsparite did not grow syntaxially on the test crystals, but rather engulfed the test. This relationship indicates that the precipitation of cement and microspar postdates what appears to be the test of the calcisphere, and we thus conclude that, in these best-preserved samples, the original ultrastructure of the test is preserved. This description fits well with that of genus *Orthopithonella* of Keupp and Mutterlose (1984), and we thus tentatively attribute all calcispheres to *Orthopithonella*. Janofske (1992) described *Orthopithonella misurinae* from the Carnian of the Dolomites, which is similar to our material in terms of wall structure and size. Moreover, the calcispheres studied by Janofske (1992) come from Misurina section in the Dolomites, which covers the onset of the CPE and is stratigraphically equivalent to the section of Milieres (see section 2.4) where the first NCIE is recorded (Dal Corso et al., 2012). However, the aperture, which is a diagnostic character of Janofske's (1992) *Orthopithonella misurinae* when compared to other *Orthopithonella*, could not be observed in our calcispheres, so an attribution at specific level is not possible. Point counting at FESEM show that 4 analysed hemipelagic limestones of the Nosztor Limestone are composed 86% to 90% of microsparite (the matrix), while calcispheres constitute 3% to 8% of the rocks (Table 1). <9% of the limestone is constituted by other skeletal components, non-carbonate elements, and syntaxial calcite overgrowth on calcispheres. No calcispheres have been observed in older limestone of the Menchley Marls member (Veszprém Fm.) and the Füred Fm. (Table 1).

4.1.2 Eastern Julian Alps, Slovenia

Calcispheres in lime mudstones from Slovenia are less common, and their morphology was characterized with less detail. Calcispheres of Mt. Škrlatica section (Slovenia) are also diagenetically overgrown, with apparently no remains of their original tests being preserved, as for "stage d" of Preto et al. (2013, their Fig. 13) (Fig. 4).

4.1.3 Western Julian Alps, Italy

Only a few calcispheres from lime mudstones of the Carnitza Fm. of the Julian Alps in North-eastern Italy were hollow spheres. The most common morphology of calcispheres from this locality are full spheres made of sub-micrometric irregular crystals, disposed irregularly. The original habit of crystals in these samples is most probably obliterated by diagenesis, and in fact, at a sub-micrometric scale, crystals of the calcispheres fit together with triple junctions and completely occlude the pore space (Fig. 4). These calcispheres have an average diameter of 8–10 μm. A few hollow specimens have a test with a thickness of ~ 1 μm. The calcispheres filled by irregular crystals that occur in the upper Carnian (Tuvalian) of the Tarvisio Basin may look like collapsed calcispheres as those of stage b in Preto et al. (2013a), but are distinct because they preserved a perfectly spherical shape. It is not possible to recognize the essential characters of *Orthopithonella* in these calcispheres, with the possible exception of a few hollow specimens (e.g., Fig. 4C). We here hypothesize that the calcipsheres of the Carnitza Fm. are *Orthopithonella* as well, which were subject to a diagenetic alteration different from the syntaxial overgrowth and collapse described by Preto et al. (2013a). This attribution of the calcispheres of the Western Julian Alps should be, however, considered only tentative and subjected to future amendments, as soon as further data become available. Point counting at FESEM of 2 samples from the Tuvalian Carnitza Fm. shows that calcispheres constitute 1 – 4% of this hemipelagic limestone (Table 1); 83 – 95% of the rock is microsparite, and 4 – 13% is other skeletal components, non-carbonate

elements, and syntaxial calcite overgrowth on calcispheres. No calcispheres have been observed in older samples so far.

4.1.4 Dolomites, Italy

The calcispheres of the Milieres section (Dolomites, Italy) in the Dolomites were only observed in thin section under a petrographic microscope, and appear as hollow spheres of few tens of μm with a radial test, which probably reflects a diagenetic overgrowth (see Preto et al. 2013a). Calcispheres are absent or rare in Late Permian to Late Triassic (Early Carnian) samples of deep water, fine grained carbonates from the Dolomites (Table 2).

4.2. Transmitted light microscope

Calcispheres were found in shales (smear slides) from the succession of the Transdanubian Range (Fig. 2 and 5 and supplementary material). They are in general rare in the few shale levels within the Füred Fm. (early Julian), but become common - abundant at the base of the Veszprém Fm., i.e., in correspondence to the first NCIE and onset of the CPE. At the light microscope, calcispheres show a certain degree of morphologic variability both in term of outline, size and microstructure. Most commonly they have a perfectly circular section but specimens with an oval shape and, more rarely, arch-shaped have been encountered. Another interesting character is the crystal size that could vary from coarse (>3 μm), to medium (1-3 μm) to fine (< 1 μm). The size of the calcispheres is variable with most of them varying from 3-5 μm to 15- 20 μm (Fig. 5). The wall of each form is composed of a mosaic of irregular interlocking elements/crystals with a similar c-axis orientation, the sutures among single crystals are usually slightly depressed. The extinction figure is thus the result of the behaviour of each individual element but also of the interaction among different crystals. The common c-axis orientation produces a virtually simultaneous extinction of each single crystal, but these individual elements are still visible and distinguishable because of the presence of the sutures that, in a way,

separates the single components. These peculiar features are particularly evident when the extinction figure of the same specimen is observed at 0°, when it is bright, and, successively, at 45° (Fig. 5).

5. Discussion

5.1 Morphology and affinity of the Carnian calcispheres

Diagenetic processes, discussed in Preto et al. (2013), may alter the pristine morphology of the calcispheres and therefore make their taxonomy difficult to assess. The main diagenetic alterations are the mechanical collapse of the calcisphere and the overgrowth of calcite cement on the calcisphere test. However, diagenetic modifications can be easily identified and disentangled from pristine morphologies (Preto et al., 2013a). Two basic morphologies of calcispheres occur in our material as observed at the SEM: hollow "spherical" calcispheres with a thin (~1 μm) test, made of calcite crystals that are radially oriented (*Orthopithonella*), and calcispheres filled by a mesh of irregular, sub-micrometric calcite crystals. Our results show that calcispheres possibly ascribable to *Orthopithonella* occur rarely in the Triassic before the CPE (Table 2), but became more abundant at the CPE (Julian 2). A third type of Late Triassic calcisphere morphology, that of *Prinsiosphaera triassica* and similar forms, has been described in Norian successions, but does not occur in our samples. *Prinsiosphaera* formed calcispheres filled by piles of thin calcite plates no larger than 1–2 μm (e.g., Bralower et al., 1991; Gardin et al., 2012; Preto et al., 2013b) and only occurs since the middle–upper Norian (Gardin et al., 2012; Demangel et al., 2020), to become a dominant element not earlier than in the Rhaetian (Preto et al., 2013b; Demangel et al., 2020).

The dimensions of the Carnian *Orthopithonella* calcispheres found in the studied sections, as measured in SEM images, are similar (~ 5–15 μm) to those found by Onoue and Yoshida (2010) in the Panthalassa deep-water succession of Japan and to the smallest of those found by Preto et al. (2013a) in the Tethys successions of Italy. As previously observed, they are in general significantly smaller than other spherical calcispheres in younger Mesozoic rocks (~ 25–100 μm; Dias-Brito, 2000; Wendler et

al., 2013). Cretaceous pithonellid calcispheres have been classified as proloculi of foraminifera, benthic or planktonic foraminifera, spores of calcareous algae, unicellular algae, planktonic algal cysts, protozoa, planktonic protists, oolitic structures, etc. (see Dias-Brito, 2000; Wendler et al., 2013). However, observation of the structure of well-preserved material and palaeoecological considerations (Dias-Brito, 2000; Wendler et al., 2013), suggest that the Cretaceous pithonellids were most likely calcareous dinoflagellates (Dias-Brito, 2000; Wendler et al., 2013). Janofske (1992) extracted from Carnian sediments of the Dolomites (Misurina Lake section, late Julian) well preserved calcispheres (*Orthopithonella misurinae*) that could be observed in three dimensions at the SEM. As previously mentioned in the Results, these calcispheres are found in a succession of the Dolomites (Italy) of the same age of those sampled in this study, and are also comparable in shape and size to the calcispheres here reported. Moreover, they present characteristics that allowed their identification as calcareous dinocysts (Janofske, 1992). Hence, by comparison of the Carnian calcispheres (i.e., *Orthopithonella*) found in the studied sections with previous studies (Janofske, 1992; Preto et al., 2013a), we interpret these calcispheres as calcareous dinoflagellates.

5.2 Rise of calcispheres during the CPE

Carnian calcispheres were known so far from the Northern Calcareous Alps, from the Dolomites, from the Lagonegro and Sicani basins of Southern Italy, and from a deep-water succession of Japan (Jafar, 1983; Janofske, 1992; Bellanca et al., 1995; Onoue and Yoshida 2010; Preto et al., 2012, 2013a). Apart for those of the Dolomites, these occurrences have a late Carnian age, and are all post-CPE. In deep-water siliceous micrite of Japan, Onoue and Yoshida (2010) found calcispheres of *Orthopithonella* and *Obliquopithonella*. The age of these calcispheres is constrained by conodont biostratigraphy of the Japanese successions to the late Carnian – middle Norian (Fig. 6) (Onoue and Yoshida, 2010). In the deep-water Lagonegro Basin, where Preto et al. (2013a) conducted their study, the carbonate sedimentation abruptly halts at the CPE and is later replaced by the deposition of shales and radiolarites

of the so-called "green clay-radiolaritic horizon" (Rigo et al., 2007; 2012). The calcispheres in the Lagonegro Basin occur in the limestones above the green clay-radiolaritic horizon, along with conodonts of early Tuvalian (late Carnian) age (Fig. 6). An ash layer within the "green clay-radiolaritic horizon" has been dated with zircon U/Pb radioisotope analysis at 230.91±0.33 Ma (Furin et al., 2006), while the CPE is currently dated at ca. 234–232 Ma on the basis of the available magnetostratigraphic and biochronostratigraphic data, and recent radiometric dating of volcanic ashes in terrestrial successions of South America (Bernardi et al., 2018; Maron et al., 2019; Sun et al., 2019; Dal Corso et al., 2020). The calcispheres from the Dolomites illustrated by Jafar (1983) and Janofske (1992) were isolated from a stratigraphic unit called "Upper Cassian Beds", which was recently the object of stratigraphic revisions (Neri et al., 2007; Gianolla et al., 2018). It corresponds to the "Unit A" of Russo et al. (1991) (cf. Gattolin et al., 2015), recently formalized by Gianolla et al. (2018) with the name of "Alpe di Specie Member" at the base of the Heiligkreuz Fm. (Fig. 1), which has a Julian 2 (early Carnian) age. The age attribution of the outcrops described by Jafar (1983) and Janofske (1992) is necessarily consequent to an *ex-post* reinterpretation. Therefore, previous data didn't allow to deduce a solid temporal and cause-and-effect relationship with the CPE, while the link is obvious in the sections considered in this study (Fig. 2 and 3).

The calcispheres in the Carnitza Fm. are late Carnian in age (e.g., De Zanche et al., 2000; Gale et al., 2015; Fig. 6), but older lithostratigraphic units of the Tarvisio Basin are shallow water, and thus calcispheres are not expected to occur, and in fact were not observed so far (Fig. 2). In other localities where early Carnian deep water units occur, the calcispheres appear much earlier. The occurrence of calcispheres at Milieres has an early Carnian, Julian 2 age (Dal Corso et al., 2012; Fig. 2), immediately after the first NCIE of the CPE. Calcispheres are very rare or absent in the late Anisian to early Carnian (Julian 1) deep-water formations of the Dolomites (e.g., Preto et al., 2009; Preto, 2012; Fig. 2 and Table 2). In the Transdanubian range (Balatonfüred), an increase of calcispheres is also coincident with the onset of the CPE and the associated C-isotope perturbations (Fig. 3 and 6). In particular, in the

marls of the Mencshely Member (Veszprém Fm.) calcispheres are common in smear slides prepared from marly lithologies (Fig. 3). In the Nosztor Limestone Member of the Veszprém Fm., calcispheres are common in FESEM images, but no calcispheres were found in the deep-water lime mudstone and wackestone of the Füred Fm., deposited before the onset of the CPE, while rare calcisphere are present in the few shales within the same formation (Fig. 3). The Nosztor Limestone Member in the Vezprem Fm., Transdanubian Range of Hungary, stands out as a thick limestone interval within hundreds of metres of marls and shales deposited during the CPE. It occurs just after the second NCIE identified in this succession, and can be considered the first limestone with significant pelagic contribution, with up to 8% of the total rock volume composed by calcispheres. After these first occurrences, similar calcispheres are present for the rest of the Carnian (Onoue and Yoshida, 2010; Preto et al., 2013a), and are abundant in the Norian and Rhaetian of the Sicani Basin, Sicily (Preto et al., 2013b). Spherical calcispheres that may belong to genus *Orthopithonella*, associated with dominant *Prinsiosphaera*, are rare but still present in the Norian and Rhaetian of the Northern Calcareous Alps (Gardin et al., 2012).

Summarizing, the new data collected for this work show that calcispheres, mostly belonging to genus *Orthopithonella* and of possibly calcareous dinoflagellate affinity, rose in the early Carnian, immediately after the onset of the CPE, when they already became an important constituent of pelagic carbonate sedimentation (Figs. 3 and 6, and Table 1). Our findings date back to the base of the Julian 2 (~234 Ma) their first occurrence as major components of hemipelagic–pelagic limestones, i.e., ~3–4 Myrs older than previously estimated. Hence, we show that there is temporal coincidence between the CPE and the first rise of *Orthopithonella* calcispheres (Fig. 6). Moreover, data suggest that these putative calcareous dinoflagellates (Janofske, 1992) spread sharply, as confirmed by slightly younger findings in other localities both in the Tethys realm and in Panthalassa (Fig. 6) (Onoue and Yoshida, 2010; Preto et al., 2013a). Unfortunately, it remains difficult to evaluate the extent of the geographical distribution of these calcispheres during the Carnian, due to the paucity of preserved deep-water carbonate successions. It is, however, remarkable that where these successions are preserved, and have

been examined for it, calcispheres are commonly found (this study and, e.g., Onoue and Yoshida, 2010).

5.3. A milestone evolutionary innovation in the Carnian?

What triggered the calcisphere acme at the CPE? In the Cretaceous, pithonellids were thermophilic plankton, which was limited to tropical shelf–shallow bathyal environments (Dias-Brito, 2000). They were opportunistic r-strategy organisms that spread in environments with high availability of carbonate (Dias-Brito, 2000). Cretaceous pithonellid calcispheres are thought to be disaster taxa, which dominate post-mass extinction nannofossil communities (e.g., Jiang et al., 2010). For example, in several Cenomanian–Turonian boundary deep-marine successions a synchronous acme of pithonellid calcispheres have been recorded, which is associated with the rise of r- or r/K strategy planktic foraminifera (Hart et al., 1991; Wendler et al., 2002, 2013a; Wilkinson, 2011; Omana et al., 2014) and has been linked to intense primary productivity due to eutrophication of the seawaters. At the Cenomanian–Turonian boundary high temperatures, C-cycle perturbation, anoxic conditions, and increased extinction rate among the marine biota are documented (Jenkyns, 2010). These environmental changes are linked to high crustal production rates and the formation of oceanic plateaus (Kerr, 1998). After the mass extinction at the Cretaceous–Palaeogene (K–Pg) boundary, one of the Big Five (e.g., Bond and Grasby, 2017), calcispheres (*Thoracosphaera* and *Orthopithonella*) dominate the nannofossil assemblages in the aftermath of the event (Jiang et al., 2010). The K–Pg mass extinction is also associated to massive environmental changes linked to the eruption of the Deccan Traps and meteorite impact (e.g., Bond and Grasby, 2017).

A possible explanation is therefore that calcispheres in the Julian 2 – Tuvalian were disaster forms related to harsh marine environmental conditions. As previously summarized, the CPE is marked by multiple injections of ^{13}C-depleted CO_2 into the Carnian atmosphere–ocean system (Dal Corso et al., 2012; 2018; Sun et al., 2016, 2019; Miller et al., 2017; Tomimatsu et al., 2021), and global

warming, recorded by $\delta^{18}O$ of conodont apatite (Sun et al., 2016). The C-isotope perturbations, in the sedimentary record, are coincident with an enhanced hydrological cycle, which resulted in an increased transport of siliciclastic material into the basins (Dal Corso et al., 2018a), and probably high discharge of nutrients into the ocean (see for example Jenkyns, 2010 for a detailed explanation of the mechanism). High extinction rates among all marine groups, including ammonoids, conodonts, bryozoa and crinoids, are documented (Simms and Ruffell, 1989; Dal Corso et al., 2020). Moreover, local anoxia has been recognised in restricted basins of the Tethys Ocean (cf. Dal Corso et al., 2018). These data indicate comparable environmental conditions to those characterizing the pithonellid acmes during the Cretaceous. However, similar extreme seawater conditions happened frequently before the CPE. Moreover, after the CPE calcispheres remained there, in similar or higher abundances, for the rest of the Carnian and most of the Norian (Onoue and Yoshida, 2010; Preto et al., 2013a, b): i.e., they seem not to be restricted to the Carnian crisis interval. Hence, the question remains: why plankton (probably dinoflagellates) started to biomineralize to such an extend only at this time of Earth's history?

The evolutionary success of planktic calcifiers in the Mesozoic was able to produce a radical revolution in ocean chemistry and ecosystem structure (e.g., Ridgwell, 2005; Suchéras-Marx et al., 2019): the transition from an ocean where carbonate precipitation was dominated by shallow-water biocalcification ("Neritan" ocean), to an ocean dominated by pelagic biocalcification ("Cretan" ocean) (Zeebe and Westbroek, 2003). Kilometres of carbonate ooze have been deposited on the floor of "Cretan" oceans, and still today constitute a major carbonate sink of carbonate production into the lithosphere, that stabilises the global C-cycle (Zeebe and Westbroek 2003; Ridgwell 2005; Ridgwell and Zeebe 2005). This mechanism is a much more efficient regulation system of the saturation state of marine calcium carbonate (Zeebe and Westbroek, 2003; Ridgwell 2005; Ridgwell and Zeebe, 2005; Goddéris et al., 2008). Our data show that some pelagic biocalcification performed by dinoflagellates was already active in the early Carnian (late Julian), and that these organisms became quickly an important component of deep-water carbonate sediments (Fig. 3), reaching widespread, if not global,

distribution (Onoue and Yoshida, 2010; Fig. 6). It is not the aim of this study to assess the impact of the Carnian calcispheres rise on the global biogeochemical cycles, and this would be anyway difficult because a real estimate of the carbonate fluxes to sediment over a significant area is not yet possible, but we argue that the beginning of the transition from a "Neritan" to a "Cretan" ocean could have started in the Carnian. The ultimate reason of this switch remains unknown.

The emergence of pelagic carbonate biomineralization in the Late Triassic could have risen as a consequence of the Permian–Triassic mass extinction (Bown et al., 2004), which wiped out 90% of marine species and 70% of terrestrial species, marking the end of the so called "Palaeozoic fauna" (Wignall, 2015). The Permian – Triassic boundary collapse of marine ecosystems would have given an evolutionary opportunity to pelagic calcifiers to thrive (Bown et al., 2004). However, as pointed out by Bown and colleagues (2004), the actual first occurrence of these organisms, in a considerable amount, happened only several (~20) million years after the Permian–Triassic mass extinction, and molecular clocks show that they were actually already there earlier, but before the Carnian they were rare or, more simply, didn't calcify. This could point to an important external causal factor, like profound changes in the global biogeochemistry of the ocean, that drove dinoflagellates first, and then other planktonic organisms, to secrete calcium carbonate tests/walls.

The CPE is marked by massive changes in the carbonate cycle: a sudden reduction of carbonate precipitation in shallow water environments, widespread change in the platform carbonate factories from microbial-dominated to metazoan-dominated (Schlager and Schöllnberger, 1974; Simms and Ruffell, 1989; Preto and Hinnov, 2003; Keim et al., 2006; Hornung et al., 2007; Stefani et al., 2010; Gattolin et al., 2015; Dal Corso et al., 2015, 2018a, 2020; Jin et al., 2019), widespread and abundant ooids formation, and abundant cement precipitation (Gattolin et al., 2015). This pattern suggests modifications in the carbonate saturation state of the Ocean. Moreover, the CPE appears to have been also coincident with another milestone event in Earth's carbonate ecosystems, i.e., when Scleractinia corals, for the first time, became dominant reef builders (e.g., Martindale et al., 2019; Dal Corso et al.,

2020). Such coincidence is intriguing and future work should concentrate on the oceanic biogeochemical conditions under which these evolutionary events happened.

Conclusions

Calcispheres of possible dinoflagellate affinity begin to be significant component of carbonate sedimentation immediately after the first negative C-isotope excursion that marks the onset of the CPE. Syn- and post-CPE limestones from deep-water successions of western Tethys, as well as previously published material from Panthalassa, yield abundant calcispheres, showing that in the Carnian the organisms producing these calcite tests reached a wide distribution quickly. Point counting on the Nosztor Limestone Member of Hungary demonstrates that these calcareous nannofossils were a significant component of hemipelagic – pelagic limestones already since the early Carnian (latest Julian, *A. austriacum* ammonoid biochronozone), i.e. during the CPE. Two basic morphologies of calcispheres occur in our material as observed at the FESEM: hollow "spherical" calcispheres with a thin (~1 μm) test wall, in which calcite crystals are radially oriented, and calcispheres filled by a mesh of irregular, sub-micrometric calcite crystals. Observations on the best-preserved material of Hungary allows us to attribute these calcispheres to *Orthopithonella*, most likely *O. misurinae* Janofske (1992), which was interpreted as calcareous dinoflagellate. The rise of calcispheres occurs at the same time of an extinction event that impacted marine fauna, and is coeval with the emergence of the first Scleractinia coral reefs and with an important change in platform carbonate factories. The coincidence between the CPE environmental changes and the emergence of significant pelagic calcification points to a causal link, and future work is needed to elucidate the biogeochemical changes that occurred at this time and favoured such deep changes in the global carbonate cycle.

Acknowledgements

JDC, NP, SH, AM and PG thank the Hanse-Wissenschaftskolleg (HWK), Institute for Advanced Study

(Delmenhorst, Germany) for funding to create the Study Group on the Carnian (coordinator: JDC). We thank T. Budai, B. Raucsik, J. Haas, G. Csillag, M. Caggiati, M. Franceschi, B. Celarc, A. Fiore and A. Montanari for their help in the field and discussions about the Triassic stratigraphy of the Julian Alps and Transdanubian Range. P. Witte (Bremen) is thanked for the professional-as-usual contribution with the FESEM. We thank the editors and three anonymous reviewers for their comments and suggestions, which greatly improved the manuscript.

Declaration of interests

The authors declare that they have no known competing financial interests or personal relationships that could have appeared to influence the work reported in this paper.

The authors declare the following financial interests/personal relationships which may be considered as potential competing interests:

References

Baranyi, V., Miller, C.S., Ruffell, A., Hounslow, M., Kürschner, W., 2019. A continental record of the Carnian Pluvial Episode (CPE) from the Mercia Mudstone Group (UK): palynology and climatic implications. Journal of the Geological Society, 176:149–166 https://doi.org/10.1144/jgs2017-150

Bellanca A, Di Stefano P, Neri R, 1995. Sedimentology and isotope geochemistry of Carnian deep-water marl/limestone deposits from the Sicani Mountains, Sicily: environmental implications and evidence from planktonic source of lime mud. Palaeogeogr Palaeoclimat Palaeoecol 114, 111–129.

Bernardi, M., Gianolla, P., Petti, F.M., Mietto, P., Gianolla, P., 2018. Dinosaur diversification linked with the Carnian Pluvial Episode. Nat. Commun. 9, 1499 doi:10.1038/s41467-018-03996-1

Bond, D.P.G., Grasby, S.E., 2017. On the causes of mass extinctions. Palaeogeogr Palaeoclimat Palaeoecol 478, 3–29.

Bown, P.R., 1992. Late Triassic-Jurassic calcareous nannofossils of the Queen Charlotte Islands, British Columbia. Journal of Micropalaeontology 11, 177–188.

Bown, P. R., & Young, J. R., 1998. Techniques. In P. R. Bown (Ed.), Calcareous nannofossil biostratigraphy, (pp. 16–28). Cambridge: Kluwer Academic Publishers.

Bown, P. R., Lees, J. A. & Young, J. R., 2004. Calcareous nannoplankton evolution and diversity through time. Coccolithophores: from molecular processes to global impact, 481–508.

Bralower TJ, Bown PR, Siesser WG, 1991. Significance of Upper Triassic nannofossils from the Southern Hemisphere (ODP Leg 122, Wombat Plateau, N.W. Australia). Mar Micropaleont 17, 119–154.

Budai, T., Császár, G., Csillag, G., Dudko, A., Koloszár, L., Majoros, G., 1999. Geology of the Balaton Highland. Occasional Papers. Geological Institute of Hungary, Budapest, p. 197.

Caggiati, M., Gianolla, P., Breda, A., Celarc, B., Preto, N., 2018. The start-up of the Dolomia Principale/Hauptdolomit carbonate platform (Upper Triassic) in the eastern Southern Alps. Sedimentology 65, 1097–1131.

Celarc, B. and Kolar-Jurkovšek, T., 2008. The Carnian–Norian basin- platform system of the Martuljek Mountain Group (Julian Alps, Slovenia): progradation of the Dachstein carbonate platform. Geol. Carpath., 59, 211– 224.

Celarc, B., Gale, L., Kolar-Jurkovšek, T., 2014 New data on the progradation of the Dachstein carbonate platform (Kamnik-Savinja Alps, Slovenia). Geologija 57/2, 095-104, doi:10.5474/geologija.2014.009

Chayes, F., 1956, Petrographic modal analysis—an elementary statistical appraisal. Wiley, New York, 139 p.

Dal Corso, J., Mietto, P., Newton, R.J., Pancost, R.D., Preto, N., Roghi, G., Wignall, P.B., 2012. Discovery of a major negative $\delta^{13}C$ spike in the Carnian (Late Triassic) linked to the eruption of Wrangellia flood basalts. Geology 40, 79–82. https://doi.org/10.1130/G32473.1.

Dal Corso, J., Gianolla, P., Newton, R.J., Franceschi, M., Roghi, G., Caggiati, M., Raucsik, B., Budai, T., Haas, J., Preto, N., 2015. Carbon isotope records reveal synchronicity between carbon cycle perturbation and the “Carnian Pluvial Event” in the Tethys realm (Late Triassic). Glob. Planet. Change 127, 79–90. https://doi.org/10.1016/j.gloplacha.2015.01.01

Dal Corso, J., Gianolla, P., Rigo, M., Franceschi, M., Roghi, G., Mietto, P., Manfrin, S., Raucsik, B., Budai, T., Jenkyns, H.C., Reymond, C.E., Caggiati, M., Gattolin, G., Breda, A., Merico, A., Preto, N., 2018a. Multiple negative carbon-isotope excursions during the Carnian Pluvial Episode (Late Triassic). Earth-Science Reviews, 185, 732–750.

Dal Corso, J., Ruffell, A., Preto, N., 2018b. The Carnian pluvial episode (Late Triassic): new insights into this important time of global environmental and biological change. Journal of the Geological Society, 175, 986–988.

Dal Corso, J., Ruffell, A., Preto, N., 2019. Carnian (Late Triassic) C-isotope excursions, environmental changes, and biotic turnover: a global perturbation of the Earth's surface system. Journal of the Geological Society, 176, 129–131, https://doi.org/10.1144/jgs2018-217

Dal Corso, J., Bernardi, M., Sun, Y., Song, H., Seyfullah, L.J., Preto, N., Gianolla, P., Ruffell, A., Kustatscher, E., Roghi, G., Merico, A., Höhn, S., Schmidt, A.R., Marzoli, A., Newton, R.J., Wignall, P.B., Benton, M.J., 2020. Extinction and dawn of the modern world in the Carnian (Late Triassic). Science Advances, 6(38):eaba0099.

De Zanche, V., Gianolla, P., Roghi, G., 2000. Carnian stratigraphy in the Raibl/Cave del Predil area (Julian Alps, Italy). Eclogae Geol. Helv. 93, 331–347.

Demangel, I., Kovacs, Z., Richoz, S., Gardin, S., Krystyn, L., Baldermann, A., Piller, W.E., 2020. Development of early calcareous nannoplankton in the late Triassic (Northern Calcareous Alps, Austria). Glob. Planet. Change, 193, 103254.

Dias-Brito, D., 2000. Global stratigraphy, palaeobiogeography and palaeoecology of Albian–Maastrichtian pithonellid calcispheres: impact on Tethys configuration. Cretaceous Research 21, 315–349.

Erba, E., 2006. The first 150 million years history of calcareous nannoplankton: Biosphere–geosphere interactions. Palaeogeography, Palaeoclimatology, Palaeoecology, 232, 237–250.

Falkowski, P.G., Katz, M.E., Knoll, A.H., Quigg, A., Rave, J.A., Schofield, O., Taylor, F.J.R., 2004.

The evolution of modern eukaryotic phytoplankton. Science, 305, 354-360.

Furin, S., Preto, N., Rigo, M., Roghi, G., Giannola, P., Crowley, J.L., Bowring, S.A., 2006. High-precision U–Pb zircon age from the Triassic of Italy: implications for the Triassic time scale and the Carnian origin of calcareous nannoplankton and dinosaurs. Geology 34, 1009–1012. https://doi.org/10.1130/G22967A.1.

Gale, L., Celarc, B., Caggiati, M., Kolar-Jurkovšek, T., Jurkovšek, B. and Gianolla, P. (2015) Development and palaeogeographic meaning of the Late Triassic basinal succession of the Tamar Valley, northern Julian Alps, Slovenia. Geol. Carpath., 66, 269 - 283.

Gardin S, Krystyn L, Richoz S, Bartolini A, Galbrun B (2012) Where and when the earliest coccolithophores? Lethaia 45, 507–523

Gattolin, G., Preto, N., Breda, A., Franceschi, M., Isotton, M., Gianolla, P., 2015. Sequence stratigraphy after the demise of a high-relief carbonate platform (Carnian of the Dolomites): Sea-level and climate disentangled. Palaeogeogr. Palaeoclimatol. Palaeoecol. 423, 1–17. https://doi.org/10.1016/j.palaeo.2015.01.017.

Gianolla, P., De Zanche, V., Roghi, G., 2003. An Upper Tuvalian (Triassic) Platform-Basin System in the Julian Alps: the Start-up of the Dolomia Principale (Southern Alps, Italy). Facies 49, 135–150.

Gianolla, P., Morelli, C., Curato, M., Siorpaes, C., 2018. *Note Illustrative della Carta Geologica d'Italia alla scala 1:50.000, Foglio 016, Dobbiaco*. ISPRA Isbn: 978-88-9311-072-3.

Góczán, F., Oravecz-Scheffer, A., Csillag, G., 1991. The stratigraphic characterization of the Cordevolian and Julian Formations of Csukréti Ravine, Balatoncsicsó. Földt. Int. Évi Jel. 1989, 241–323.

Goddéris, Y., Donnadieu, Y., Vargas, C. D. & Pierrehumbert, R. T., 2008. Causal or casual link between the rise of nannoplankton calcification and a tectonically-driven massive decrease in Late Triassic atmospheric CO_2? Earth and Planetary Science Letters 267, 247–255.

Greene, A.R., Scoates, J.S., Weis, D., Katvala, E.C., Israel, S., Nixon, G.T., 2010. The architecture of

oceanic plateaus revealed by the volcanic stratigraphy of the accreted Wrangellia oceanic plateau. Geosphere 6, 47–73. http://dx.doi.org/10.1130/GES00212.1.

Hart, M.B., 1991, The Late Cenomanian calcisphere global bioevent: Proceedings of the Ussher Society 7, 413–417.

Hornung, T., Krystyn, L., Brandner, R., 2007. A Tethys-wide mid-Carnian (Upper Triassic) carbonate productivity crisis: Evidence for the Alpine Reingraben Event from Spiti (Indian Himalaya)? J. Asian Earth Sci. 30, 285–302. https://doi.org/10.1016/j.jseaes.2006.10.001.

Jafar, S.A., 1983. Significance of Late Triassic calcareous nannoplankton from Austria and Southern Germany. N Jb Geol Paläont Abh 166, 218–259

Janofske, D., 1992. Kalkiges Nannoplankton, insbesondere Kalkige Dinoflagellaten-Zysten der alpinen Ober-Trias: Taxonomie, Biostratigraphie und Bedeutung fur die Phylogenie der Peridiniales. Berliner Geowissenschaftliche Abhandlungen Reihe E 4, 53.

Jenkyns, H.C., 2010. Geochemistry of oceanic anoxic events. Geochem. Geophys. Geosyst. 11 (3), Q03004. https://doi.org/10.1029/2009GC002788.

Jiang, S., Bralower, T., Patzkowsky, M. et al. Geographic controls on nannoplankton extinction across the Cretaceous/Palaeogene boundary. Nature Geosci 3, 280–285 (2010) doi:10.1038/ngeo775

Jin, X., McRoberts, C.A., Shi, Z., Mietto, P., Rigo, M., Roghi, G., Manfrin, S., Franceschi, M., Preto, N., 2019. The aftermath of the CPE and the Carnian/Norian transition in northwestern Sichuan Basin, South China. Journal of the Geological Society, 176, 79-196. https://doi.org/10.1144/jgs2018-104

Jin, X., Gianolla, P., Shi, Z., Franceschi, M., Caggiati, M., Du, Y., Preto, N., 2020. Synchronized changes in shallow water carbonate production during the Carnian Pluvial Episode (Late Triassic) throughout Tethys. Global and Planetary Change 184, https://doi.org/10.1016/j.gloplacha.2019.103035

Keim, L., Spötl, C., Brandner, R., 2006. The aftermath of the Carnian carbonate platform demise: a

basinal perspective (Dolomites, Southern Alps). Sedimentology 53, 361–386. https://doi.org/10.1111/j.1365-3091.2006.00768.x.

Kerr, A. C., 1998. Oceanic plateau formation: a cause of mass extinction and black shale deposition around the Cenomanian-Turonian boundary. Journal of the Geological Society (London), 155, 619–626.

Keupp, H., & Mutterlose, J. (1984). Organismenverteilung in den D-Beds von Speeton (Unterkreide, England) unter besonderer Berücksichtigung der kalkigen Dinoflagellaten-Zysten. *Facies*, *10*(1), 153-177.

Krystyn, L., 1978. Eine neue Zonengliederung im alpin-mediterranen Unterkarn. Schrift. Erdwiss. Komm. Österr. Ak. Wiss. 4, 37–75.

Lukeneder, S., Lukeneder, A., 2015. A new ammonoid fauna from the Carnian (Upper Triassic) Kasimlar Formation of the Taurus Mountains (Anatolia, Turkey). Palaeontology 57, 357–396.

Lukeneder, S., Lukeneder, A., Harzhauser, M., Islamoglu, Y., Krystyn, L., Lein, R., 2012. A delayed carbonate factory breakdown during the Tethyan-wide Carnian Pluvial Episode along the Cimmerian terranes (Taurus, Turkey). Facies 58, 279–296. https://doi.org/10.1007/s10347-011-0279-8.

Maron, M., Muttoni, G., Rigo, M., Gianolla, P., Kent, D.V., 2019. New magnetobiostratigraphic results from the Ladinian of the Dolomites and implications for the Triassic geomagnetic polarity timescale Palaeogeogr. Palaeoclimatol. Palaeoecol., 517, 52–73.

Martindale, R.C., Foster W.J.§, Velledits F., 2019. The survival, recovery, and diversification of metazoan reef ecosystems following the end-Permian mass extinction event. Palaeogeography, Palaeoclimatology, Palaeoecology. 513, 100–115. doi: 10.1016/j.palaeo.2017.08.014.

Mastandrea, A., 1994. Carnian conodonts from Upper Triassic strata of Tamarin section (San Cassiano Fm., Dolomites, Italy). Riv. It. Paleont. Strat. 100, 493–510.

Miller, C.S., Peterse, F., da Silva, A.-C., Baranyi, V., Reichart, G.J., Kürschner, W., 2017.

Astronomical age constraints and extinction mechanisms of the Late Triassic Carnian crisis. Sci. Rep. 2557. https://doi.org/10.1038/s41598-017-02817-7.

Mueller, S., Krystyn, L., Kürschner, W.M., 2016a. Climate variability during the Carnian Pluvial Phase – a quantitative palynological study of the Carnian sedimentary succession at Lunz am See, Northern Calcareous Alps, Austria. Palaeogeogr. Palaeoclimatol. Palaeoecol. 441, 198–211. https://doi.org/10.1016/j.palaeo.2015.06.008.

Mueller, S., Hounslow, M.W., Kürschner, W.M., 2016b. Integrated stratigraphy and palaeoclimate history of the Carnian Pluvial Event in the Boreal realm; new data from the Upper Triassic Kapp Toscana Group in central Spitsbergen (Norway). J. Geol. Soc. 173, 186–202. https://doi.org/10.1144/jgs2015-028.

Munnecke, A., Servais, T., 2008. Palaeozoic calcareous plankton: evidence from the Silurian of Gotland. Lethaia 41:185–194.

Neri, C., Gianolla, P., Furlanis, S., Caputo, R., Bosellini, A., 2007. Note Illustrative della Carta Geologica d'Italia alla scala 1:50.000, Foglio 029 Cortina d'Ampezzo. SystemCart (200 p). A.P.A.T, Roma.

Omaña, L., Torres, J.R., Lopez Doncel, L., Alencáster, G., López Caballero, I., 2014. A pithonellid bloom in the Cenomanian-Turonian boundary interval from Cerritos in the western Valles–San Luis Potosí platform, Mexico: Paleoenvironmental significance. Revista Mexicana De Ciencias Geológicas 31, 28–44.

Onoue, T., Yoshida, A., 2010. Depositional response to the Late Triassic ascent of calcareous plankton in pelagic mid-oceanic plate deposits of Japan. Journal of Asian Earth Sciences, 37:312–321.

Preto, N., Hinnov, L., 2003. Unravelling the origin of carbonate platform cyclothems in the Upper Triassic Durrenstein Formation (Dolomites, Italy). J. Sediment. Res. 73, 774–789. https://doi.org/10.1306/030503730774.

Preto, N., Spötl, C., Guaiumi, C., 2009. Evaluation of bulk carbonate $\delta^{13}C$ data from Triassic

hemipelagites and the initial composition of carbonate mud. Sedimentology 56, 1329–1345.

Preto, N., Willems, H., Guaiumi, C. & Westphal, H., 2013a. Onset of significant pelagic carbonate accumulation after the Carnian Pluvial Event (CPE) in the western Tethys. Facies 59, 891–914.

Preto, N., Agnini, C., Rigo, M., Sprovieri, M. & Westphal, H., 2013b. The calcareous nannofossil Prinsiosphaera achieved rock-forming abundances in the latest Triassic of western Tethys: Consequences for the $\delta^{13}C$ of bulk carbonate. Biogeosciences 10, 6053–6068 (2013).

Ridgwell, A., Zeebe, R.E., 2005. The role of the global carbonate cycle in the regulation and evolution of the Earth system. Earth Planet Sci Lett 234, 299–315.

Ridgwell, A., 2005. A mid Mesozoic revolution in the regulation of ocean chemistry. Mar Geol 217, 339–357.

Rigo, M., Preto, N., Roghi, G., Tateo, F., Mietto, P., 2007. A rise in the Carbonate Compensation Depth of western Tethys in the Carnian (Late Triassic): deep-water evidence for the Carnian Pluvial Event. Palaeogeogr. Palaeoclimatol. Palaeoecol. 246, 188–205.

Rigo, M., Preto, N., Franceschi, M., Guaiumi, C., 2012. Stratigraphy of the Carnian -Norian Calcari con Selce formation in the Lagonegro Basin, Southern Apennines. Riv Ital Paleont Stratigr 118, 143–154.

Roghi, G., Gianolla, P., Minarelli, L., Pilati, C., Preto, N., 2010. Palynological correlation of Carnian humid pulses throughout western Tethys. Palaeogeogr. Palaeoclimatol. Palaeoecol. 290, 89–106. https://doi.org/10.1016/j.palaeo.2009.11.006.

Rostási, Á., Raucsik, B., Varga, A., 2011. Palaeoenvironmental controls on the clay mineralogy of Carnian sections from the Transdanubian Range (Hungary). Palaeogeogr. Palaeoclimatol. Palaeoecol. 300, 101–112. https://doi.org/10.1016/j.palaeo.2010.12.013.

Russo, F., Neri, C., Mastandrea, A., Baracca, A., 1997. The mudmound nature of the Cassian platform margins of the Dolomites. A case history: the Cipit boulders from Punta Grohmann (Sasso Piatto Massif, Northern Italy). Facies 36, 25–36. https://doi.org/10.1007/BF02536875.

Schlager, W., Schöllnberger, W., 1974. Das Prinzip stratigraphischer Wenden in der Schichtfolge der Nördlichen Kalkalpen. Mitt. Österr. Geol. Ges. 66–67 (165–193).

Simms, M.J., Ruffell, A.H., 1989. Synchroneity of climatic change and extinctions in the Late Triassic. Geology 17, 265–268.

Stefani, M., Furin, S., Gianolla, P., 2010. The changing climate framework and depositional dynamics of the Triassic carbonate platforms from the Dolomites. Palaeogeogr. Palaeoclimatol. Palaeoecol. 290, 43–57. https://doi.org/10.1016/j.palaeo.2010.02.018.

Suchéras-Marx, B., Mattioli, E., Allemand, P., Giraud, F., Pittet, B., Plancq, J., Escarguel, G., 2019. The colonization of the oceans by calcifying pelagic algae. Biogeosciences 16, 2501–2510. https://doi.org/10.5194/bg-16-2501-2019

Sun, Y., Wignall, P., Joachimski, M.M., Bond, D.P.G., Grasby, S.E., Lai, X.L., Wang, L.N., Zhang, Z.T., Sun, S., 2016. Climate warming, euxinia and carbon isotope perturbations during the Carnian (Triassic) Crisis in South China. Earth Planet. Sci. Lett. 444, 88–100. https://doi.org/10.1016/j.epsl.2016.03.037.

Sun, Y.D., Richoz, S., Krystyn, L., Zhang, Z.T., Joachimski, M., 2019. Perturbations in the carbon cycle during the Carnian Humid Episode: carbonate carbon isotope records from southwestern China and northern Oman. Journal of the Geological Society, 176, 167-177. https://doi.org/10.1144/jgs2017-170

Tomimatsu, Y., Nozaki, T., Sato, H., Takaya, Y., Kimura, J.-I., Chang, Q., Naraoka, H., Rigo, M., Onoue, T., 2021. Marine osmium isotope record during the Carnian "pluvial episode" (Late Triassic) in the pelagic Panthalassa Ocean. Global and Planetary Change, 197, 103387. https://doi.org/10.1016/j.gloplacha.2020.103387

Wendler, J.E., Bown, P., 2013, Exceptionally well-preserved Cretaceous microfossils reveal new biomineralization styles: Nature Communications 4. doi:10.1038/ncomms 3052.

Wendler, J.E., Gräfe, K.U., Willems, H., 2002b, Paleoecology of calcareous dinoflagellate cysts in the

mid-Cenomanian Boreal Realm: implications for the reconstruction of paleoceanography of the NW European shelf sea: Cretaceous Research, 23, 213-229.

Wendler, J.E., Wendler, I.., Huber, B.T., 2013. Revision and evaluation of the systematic affinity of the Calcitarch genus Pithonella based on exquisitely preserved Turonian material from Tanzania: Journal of Paleontology, 87(6), 1077-1106.

Wignall, P.B., 2015. *The Worst of Times*. Princeton University Press, p. 224.

Wilkinson, I.P., 2011. Pithonellid blooms in the Chalk of the Isle of Wight and their biostratigraphical potential. Proceedings of the Geologists' Association, 122, 862–867.

Zeebe RE, Westbroek P (2003) A simple model for the $CaCO_3$ saturation state of the ocean: the "Strangelove", the "Neritan", and the "Cretan" Ocean. Geochem. Geophys. Geosys. 4 (1104):26.

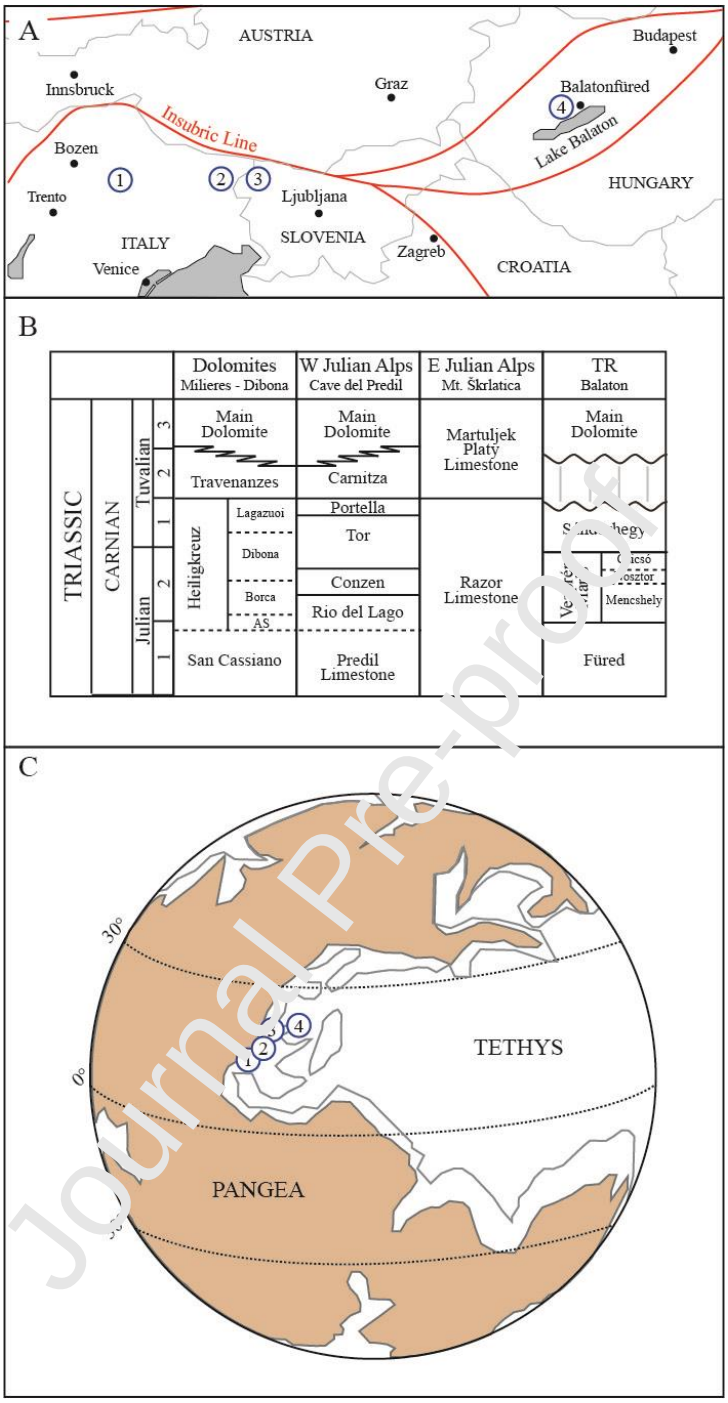

Figure 1. A) Location of the studied stratigraphic sections: 1 = Milieres, Dolomites; 2 = Cave del Predil, Western Julian Alps; 3 = Mt. Škrlatica, Eastern Julian Alps; 4 = Balatonfüred (Csukrét Section and boreholes BFU-1 and MET-1). B) Lithostratigraphic scheme of the formations in the studied areas. Biostratigraphic constraints are from Gale et al. (2015), Dal Corso et al. (2018) and references therein. Julian 1 = *Trachyceras* ammonoid Zone, Julian 2 = *Austrotrachyceras austriacum* ammonoid Zone, Tuvalian 1 = *Tropites dilleri* ammonoid Zone, Tuvalian 2 = *Tropites subbullatus* ammonoid Zone, Tuvalian 3 = *Anatropites spinosus* ammonoid Zone. TR = Transdanubian Range. C) Palaeogeographic position of the studied sections. Modified after Dal Corso et al. (2018a).

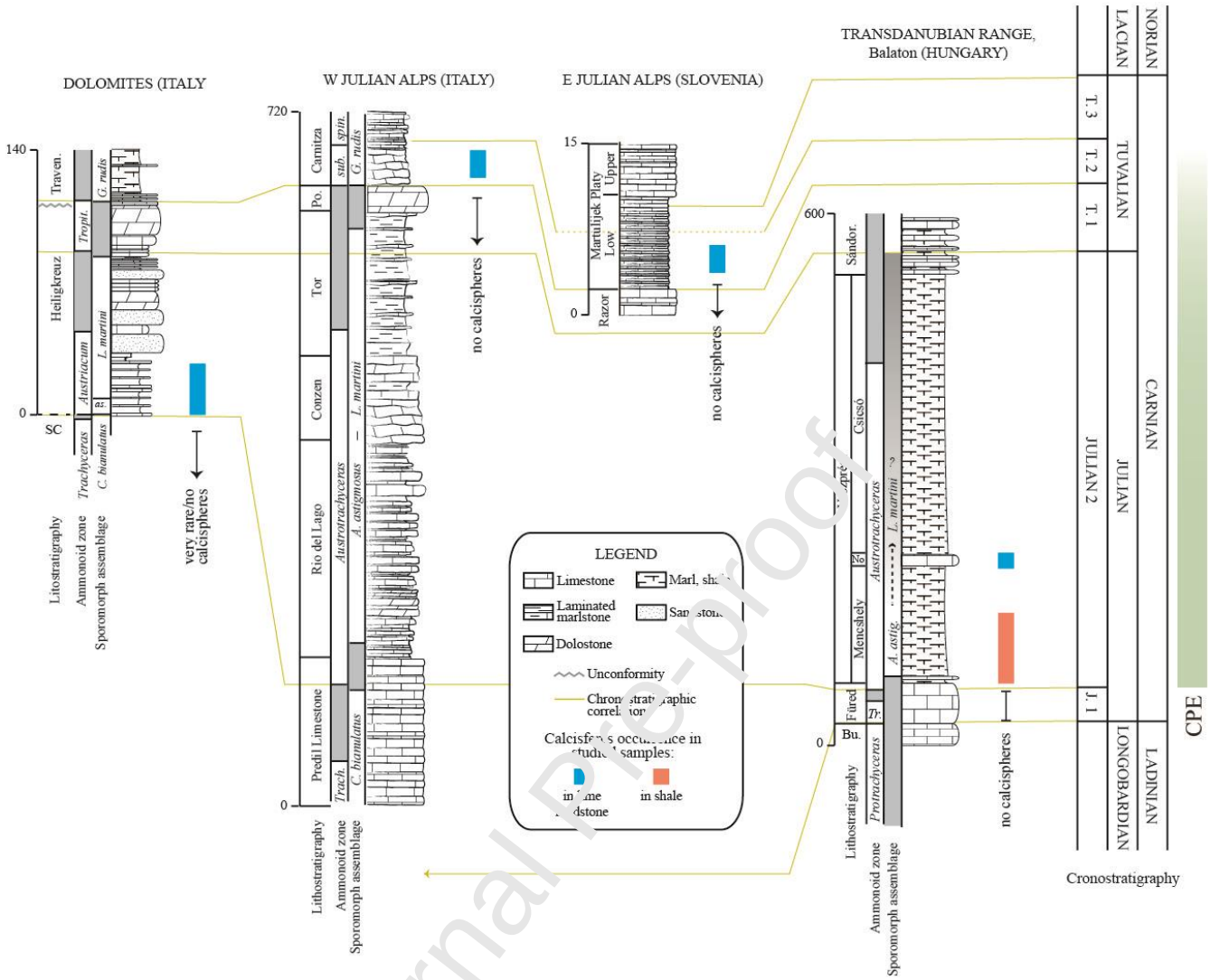

Figure 2. Occurrence of calcispheres in the studied successions. Stratigraphic logs and biostratigraphic constraints are from Dal Corso et al. (2018) and Jin et al. (2020). Dark grey areas in the biostratigraphic zonations represent intervals of uncertain biostratigraphic attribution. Abbreviations: J. = Julian; T. = Tuvalian; SC = San Cassiano Formation; Traven. = Travenanzes Formation; Po. = Portella Limestone; Sandor = Sándorhegy Formation; No = Nosztor Limestone; *Aust.* = *A. austriacum*; *Trach.* And *Tr.* = *Trachyceras*; *Tropit.* = *Tropites*; *sub.* = *Subbulatus*; *spin.* = *Spinosus*; *A. as.* = *A. astigmosus*; *L. mar* = *L. martini*.

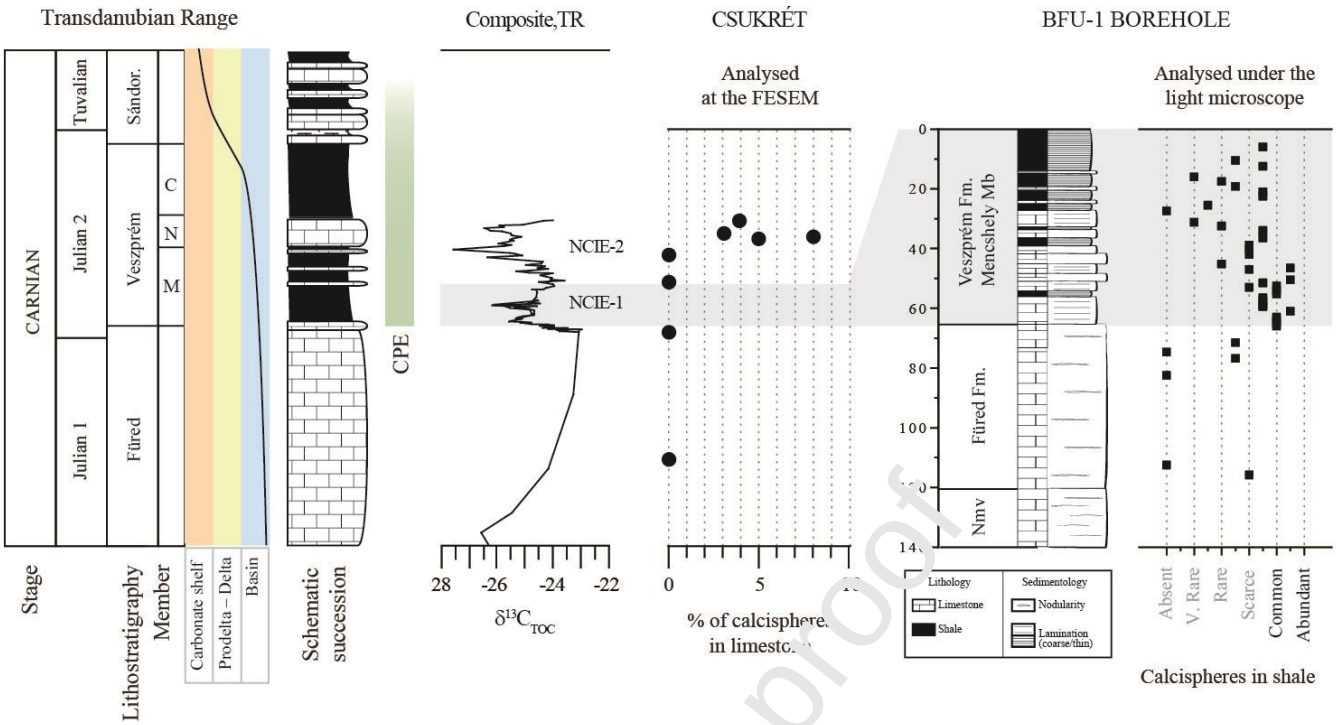

Figure 3. Abundance of the calcispheres in the succession of the Transdanubian Range and relationship with the C-isotope record. Relative abundance of calcispheres in limestone from Csukrét section and BFÜ-1 core against the composite bulk organic C-isotope curve for the Transdanubian range (Dal Corso et al., 2015, Dal Corso et al., 2018a), and occurrence and estimated abundance of calcispheres in the shales (smear slides) collected from the BFÜ-1 core. In the shales, calcispheres become common in correspondence to the NCIE, which marks the onset of the CPE. In the limestone, calcisphere s reaches 8% abundance in the Nosztor Limestone, at the second recorded NCIE, while in older limestone (Füred Fm.) they are totally absent. Note that the succession is shallowing upward, therefore calcispheres are not present going stratigraphically upward. The limestone samples were studied at the FESEM (Fig. 2) and the smear slides were studied under the light transmitted microscope (Fig. 3). Abundance determined in smear slides is defined as follows: Abundant (>10–100 specimens per field of view); Common (>1–10 specimens per field of view); Scarce (1 specimen per 1–10 fields of view); Rare (<1 specimen per 10 fields of view); Very rare (<5 specimens seen while logging slide).

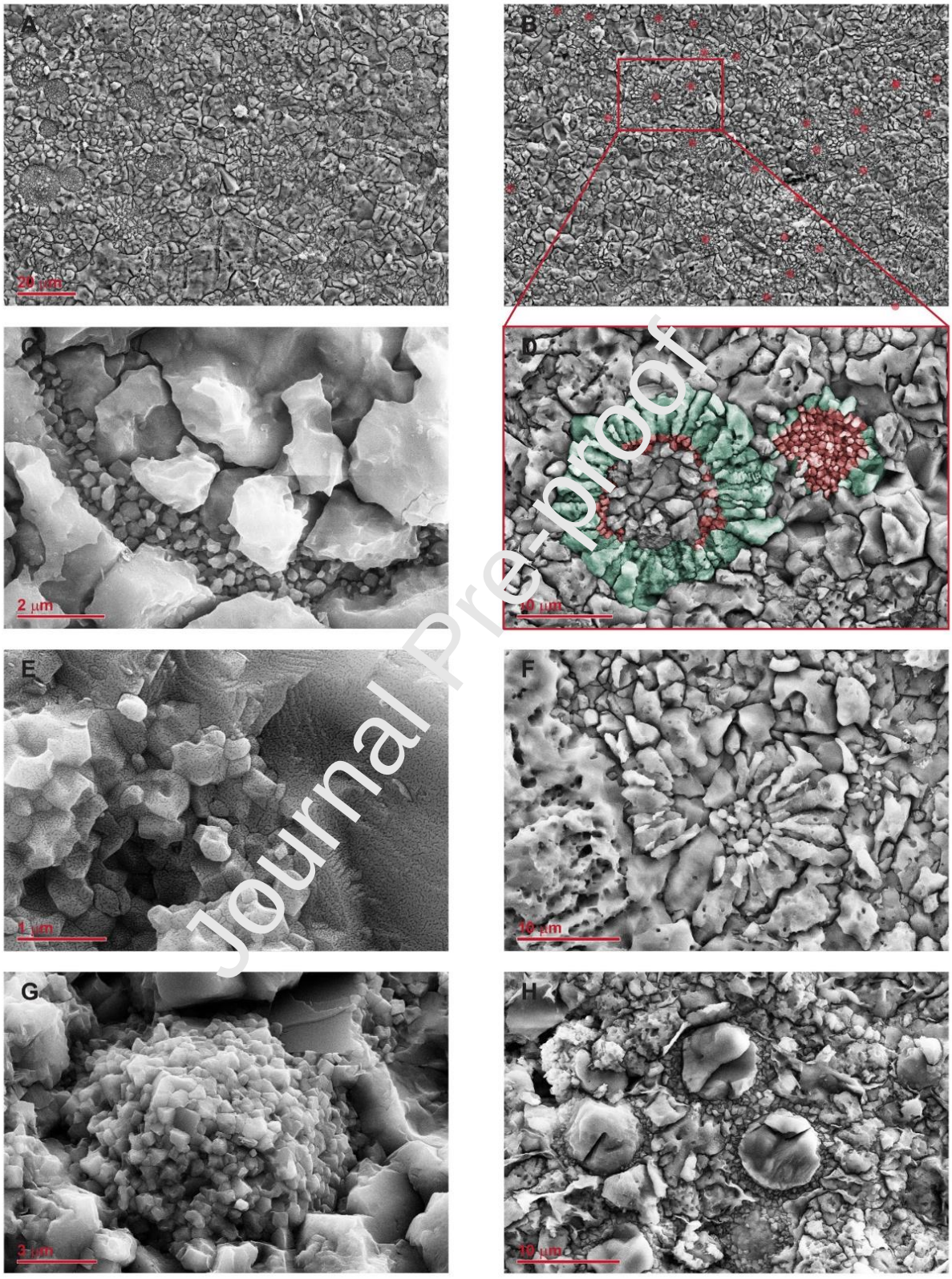

Figure 4 (previous page). Carnian calcispheres as seen at the SEM. A) Large field view of a sample with abundant filled calcispheres. Sample SC 74, Carnitza Formation of Portella Pass (Tarvisio), polished and etched. B) Large field view of a sample with abundant hollow calcispheres, highlighted by red dots. Sample CS 25, Nosztor Limestone Member of the Balaton area (Hungary), polished and etched. C) Detail of the wall of a hollow calcisphere from the Carnitza Formation of Portella Pass (Tarvisio), sample SC 74, polished and etched. D) Two calcispheres with some calcite overgrowth, which has been highlighted with water blue colour. The original wall crystals are instead highlighted in red. This image is a detail of (B). E) Detail of sub-micrometric crystals that make a filled calcisphere, which highlight the absence of pore space between the crystals and some triple junctions, implying that some diagenetic overgrowth occurred and the original shape of the crystals is lost. Sample SC 76 from the Carnitza Formation of Portella Pass (Tarvisio). F) Hollow calcisphere with external diagenetic overgrowth from the Martuljek platy limestone of Mount Škrlatica section, Slovenia. This sample (MK 06) was polished and etched. G) A calcisphere with very limited or no overgrowth from the Nosztor Limestone Member of the Balaton area (Hungary). Sample CC 04. H) A cluster of 4 hollow calcispheres from the Nosztor Limestone Member of the Balaton area (Hungary). Sample CC 07, polished and etched.

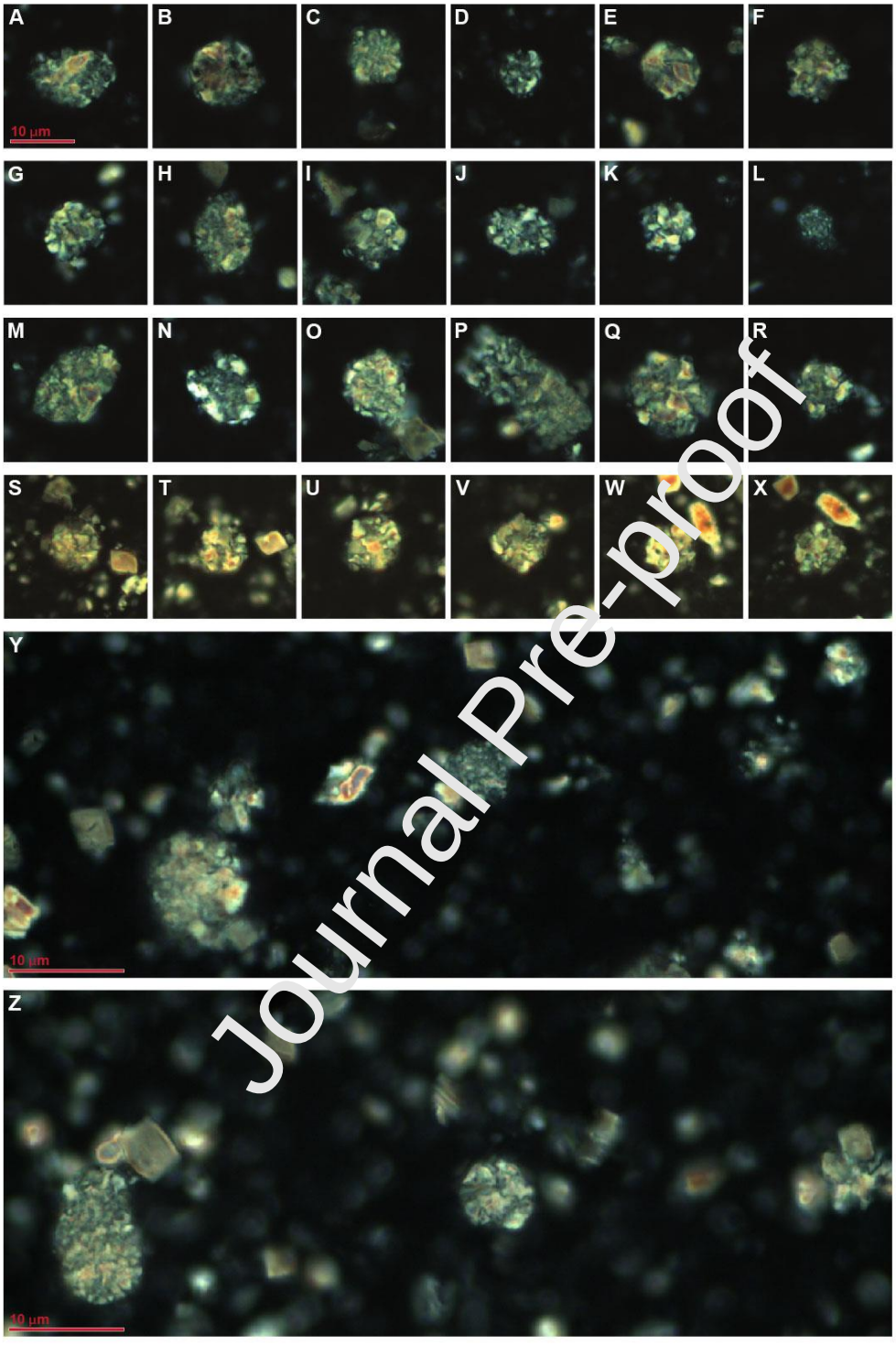

Figure 5 (previous page). Carnian calcispheres from the Transdanubian Range (Hu) as observed at the polarized light transmission microscope, crossed nicols. **A-F, S-Y**: sample Bfu-1; **G-I, Z**: sample SZBF_35bis. Calcispheres can be distinguished by their shape which could be spherical (e.g.: **B, C-E, G, I, K-L**), oval (**A, H, J, M-N**) or tubiform (**P**); and by crystal size, coarse (**B, E, Q**), medium (**A, C-K, M-P**) or fine (**L, R**). Calcispheres are distinct from generic crystal aggregates because all crystals get extinct at the same time as the plate is rotated (**S-X**) and because abiotic crystals in the smear slide samples are all coarser and mostly isolated (**Y-Z**).

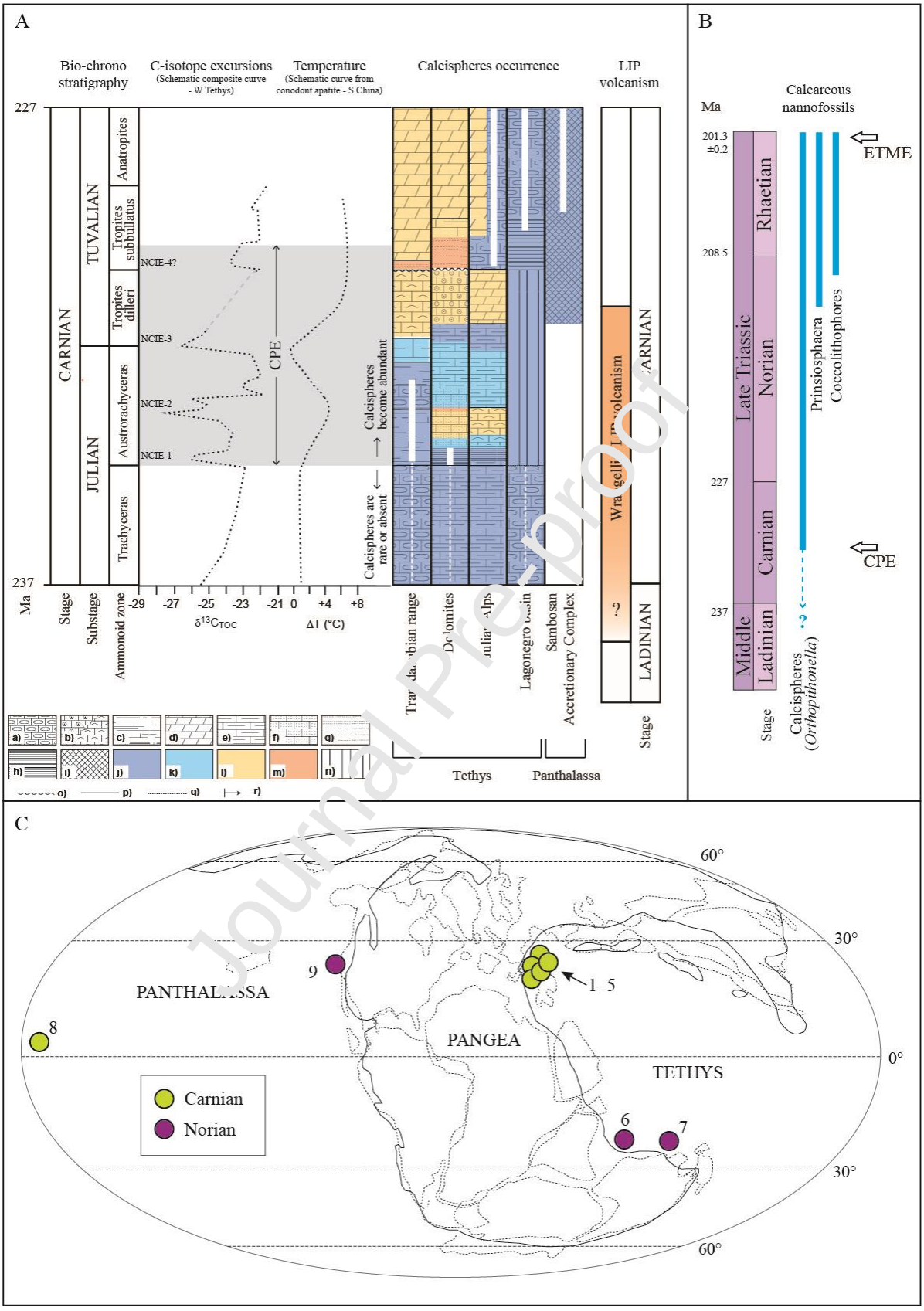

Figure 6. (previous page) A) Occurrence of calcispheres from the studied successions (white lines), and from Preto et al. (2013a; Lagonegro) and Onoue and Yoshida (2010; Sambosan Accretionary Complex). *Orthopithonella* and related calcispheres started to be an important constituent of deep-water carbonate sedimentation from the latest Julian, following the onset of the CPE. Calcispheres are present as a rare element in shale of the Transdanubian Range, (this study) at least from the early Carnian (see also Fig. 5), but they are not found in coeval limestone (Füred Fm.). In the Lagonegro Basin, calcispheres are rare in pre-CPE cherty limestone (Preto et al., 2013a). Lithologies: a) limestone, cherty limestone; b) oolitic-bioclastic limestone; c) marlstone and claystone; d) dolostone; e) marly limestone; f) sandy limestone; g) siltstone, sandstone; h) platy shales, black shales i) chert/siliceous shale; j) Abyssal, Pro-delta open shelf, Outer ramp; k) Middle ramp/outer ramp; l) Inner ramp, shallow water carbonate platform and slopes; m) continental, marginal marine; n) hiatus o) unconformity p) lithostratigraphic boundary; q) submarine unconformity; r) Calcispheres increase/appearance. The estimated maximum age span of the Wrangellia basalts in the figure is constrained by biostratigraphy (Greene et al., 2010; Dal Corso et al., 2020). C-isotope schematic composite curve is from Dal Corso et al. (2018) and is based on data from the Dolomites (Italy), the Julian Alps (Italy), the Northern Calcareous Alps (Austria), and the Transdanubian Range (Hungary). Palaeotemperature estimates are from conodont $\delta^{18}O$ data from South China (Sun et al., 2016). B) Occurrence of the main Triassic calcareous nannofossils, after Onoue and Yoshida (2010). CPE = Carnian Pluvial Episode; ETME = end-Triassic mass extinction. C) Palaeogeographical distribution of *Orthopithonella* and *Prinsiosphaera* calcispheres in the Carnian (Julian 2) – Norian, Late Triassic. The age indicates their first appearance as significant elements of hemipelagic–pelagic limestones. 1–5) North-Western Tethys successions examined in this study (Fig. 1), and in Jafar (1983) and Janofske (1992) (Dolomites), and Preto et al. (2013a) (Lagonegro Basin). 6) Wombat plateau, Australia (Bralower et al., 1991); 7) Timor (Bown, 1992); 8) Sambosan Accretionary Complex, Japan (Onoue and Yoshida, 2010); 9) Haida Gwaii (previously known as Queen Charlotte Islands), British Columbia (Bown, 1992). Modified after Onoue and Yoshida (2010). In the latest Triassic, coccolithophores also appeared (Gardin et al., 2012).

Table 1. Abundance of calcispheres in lime mudstone samples from the Transdanubian Range (TDR; Hungary) and Western Julian Alps (WJA; Italy). See also Fig. 4 and Fig. 5. The samples in the table were studied at the FESEM.

SAMPLE	% CALCISPHERES	FORMATION (Member)	AGE	SECTION	AREA
SZBF80	0	Füred	Julian 1	BFÜ-1	TDR
CC1	0	Füred	Julian 1	Csukrét	TDR
CC2	0	Veszprém (Mencshely Marl)	Julian 2	Csukrét	TDR
CS19	0	Veszprém (Mencshely Marl)	Julian 2	Csukrét	TDR
CC4	3	Veszprém (Nosztor Limestone)	Julian 2	Csukrét	TDR
CS24	5	Veszprém (Nosztor Limestone)	Julian 2	Csukrét	TDR
CS25	8	Veszprém (Nosztor Limestone)	Julian 2	Csukrét	TDR
CC7	4	Veszprém (Nosztor Limestone)	Julian 2	Csukrét	TDR
SC14	0	Predil Limestone	Julian 1	Rio Conzen	WJA
SC74	4	Carnitza	Tuvalian 2	Portella Pass	WJA
SC76	1	Carnitza	Tuvalian 2	Portella Pass	WJA

Table 2. Occurrence of calcispheres in pre-CPE formations of the Dolomites, Italy. The limestone samples were studied at the FESEM.

AGE	FORMATION	CALCISPHERES
Late Permian	Bellerophon, Werfen	absent
Lower Triassic	Werfen	very rare and uncertain
Anisian (Pelsonian)	Dont, Gracilis	absent
Anisian (Illirian)	Morbiac	absent
Anisian - Ladinian (Illirian - Fassanian)	Bivera, Ambata, Livinallongo	very rare – rare
Ladinian (Fassanian)	Livinallongo	absent
Ladinian (Longobardian)	Aquatona, Fernazza, Wengen	absent – rare

Carnian (Julian 1)	San Cassian	rare

APPENDICES

Photo		Microspar	Calcisphere	Syntaxial overgrowth	Microspar within calcisphere	Syntaxial ingrowth	Other skeletal	Non carbonate		Microspar	Calcisphere	Syntaxial overgrowth	Microspar within calcisphere	Syntaxial ingrowth	Other skeletal	Non carbonate
		Counts (% based on 500 points)								Average						
										(st.deviations)						
TDR																
SZBF 80		No calcispheres are visible with SEM									**0.0**					
CS 19		No calcispheres are visible with SEM									**0.0**					
CS 21		No calcispheres are visible with SEM									**0.0**					
CS 24 1		90.2	2.8	0.0	0.0	0.0	0.0	7.0								
CS 24 2		89.8	5.6	1.8	1.2	0.0	0.0	1.6								
CS 24 3		84.6	10.4	2.4	2.4	0.0	0.0	0.2								
CS 24 5		88.4	4.0	2.0	0.6	0.0	0.0	5.0								
CS 24 6		86.2	3.8	2.2	1.2	0.0	0.2	6.4		88.3	**5.0**	1.5	1.0	0.0	0.0	4.2
CS 24 7		90.6	3.6	0.4	0.6	0.0	0.0	4.8		*2.4*	*2.8*	*1.0*	*0.8*	*0.0*	*0.1*	*2.7*
CS 25 1		84.2	9.0	6.0	0.8	0.0	0.0	0.0								
CS 25 3		87.2	4.0	4.8	1.0	0.0	3.0	0.0								
CS 25 4		87.6	7.6	3.2	0.2	0.0	0.0	1.4								
CS 25 5		87.6	7.0	3.0	0.2	0.0	2.2	0.0								
CS 25 6		85.2	11.4	2.6	0.8	0.0	0.0	0.0								
CS 25 8		87.6	8.6	3.2	0.4	0.0	0.0	0.2		86.4	**7.9**	4.1	0.6	0.0	0.7	0.3
CS 25 9		85.2	8.0	5.6	0.8	0.0	0.0	0.4		*1.5*	*2.2*	*1.4*	*0.3*	*0.0*	*1.3*	*0.5*
CC 01		No calcispheres are visible with SEM									**0.0**					
CC 04 2		91.8	3.4	0.0	2.4	0.0	1.6	0.8								
CC 04 3		91.2	3.4	0.0	2.2	0.0	2.0	1.2								
CC 04 4		79.0	3.8	0.0	1.0	0.2	11.2	4.8								
CC 04 5		95.8	1.8	0.0	0.6	0.2	1.0	0.6		90.1	**2.9**	0.0	1.7	0.1	3.6	1.6

CC 04 6		92.6	2.2	0.0	2.4	0.0	2.0	0.8		*6.4*	*0.9*	*0.0*	*0.9*	*0.1*	*4.3*	*1.8*
CC 07 1		87.6	4.6	0.0	0.4	0.0	0.0	7.4								
CC 07 2		87.6	4.4	0.0	3.4	0.0	0.0	4.6								
CC 07 3		85.4	4.0	0.0	3.8	0.0	1.0	5.8								
CC 07 4		91.4	3.4	0.0	3.6	0.0	0.0	1.6								
CC 07 5		81.8	4.2	0.0	3.6	0.0	2.6	7.8		87.4	**3.7**	0.0	2.7	0.0	1.0	5.2
CC 07 6		90.6	1.8	0.0	1.4	0.0	2.2	4.0		*3.5*	*1.0*	*0.0*	*1.4*	*0.0*	*1.2*	*2.3*
WJA																
SC 14		No calcispheres are visible with SEM									**0.0**					
SC 74 1		74.6	3.6	0.0	0.0	0.0	21.6	0.2								
SC 74 2		79.6	3.8	0.6	0.0	0.0	12.0	4.0								
SC 74 3		91.0	2.4	0.0	0.0	0.0	3.2	3.4								
SC 74 4		87.4	4.6	3.0	1.0	0.0	3.8	0.2								
SC 74 8		88.2	3.2	0.4	0.0	0.0	8.2	0.0		82.6	**3.9**	1.0	0.2	0.0	10.6	1.5
SC 74 10		76.0	5.6	1.8	0.4	0.0	14.8	1.4		*6.9*	*1.1*	*1.2*	*0.4*	*0.0*	*7.0*	*1.8*
SC 76 2		96.4	1.6	0.0	0.0	0.2	1.8	0.0								
SC 76 4		98.8	1.2	0.0	0.0	0.0	0.0	0.0								
SC 76 5		89.6	0.8	5.6	0.0	0.0	1.6	2.4								
SC 76 6		94.8	2.4	1.8	0.0	0.0	0.0	1.0								
SC 76 8		90.8	1.0	1.2	0.2	0.0	0.0	6.8		94.8	**1.4**	1.4	0.0	0.0	0.6	1.7
SC 76 9		98.6	1.2	0.0	0.0	0.0	0.2	0.0		*3.9*	*0.6*	*2.2*	*0.1*	*0.1*	*0.9*	*2.7*

Table A1. Point counting on lime mudstones from the Transdanubian Range (TDR; Hungary) and the Western Julian Alps (WJA; Italy).

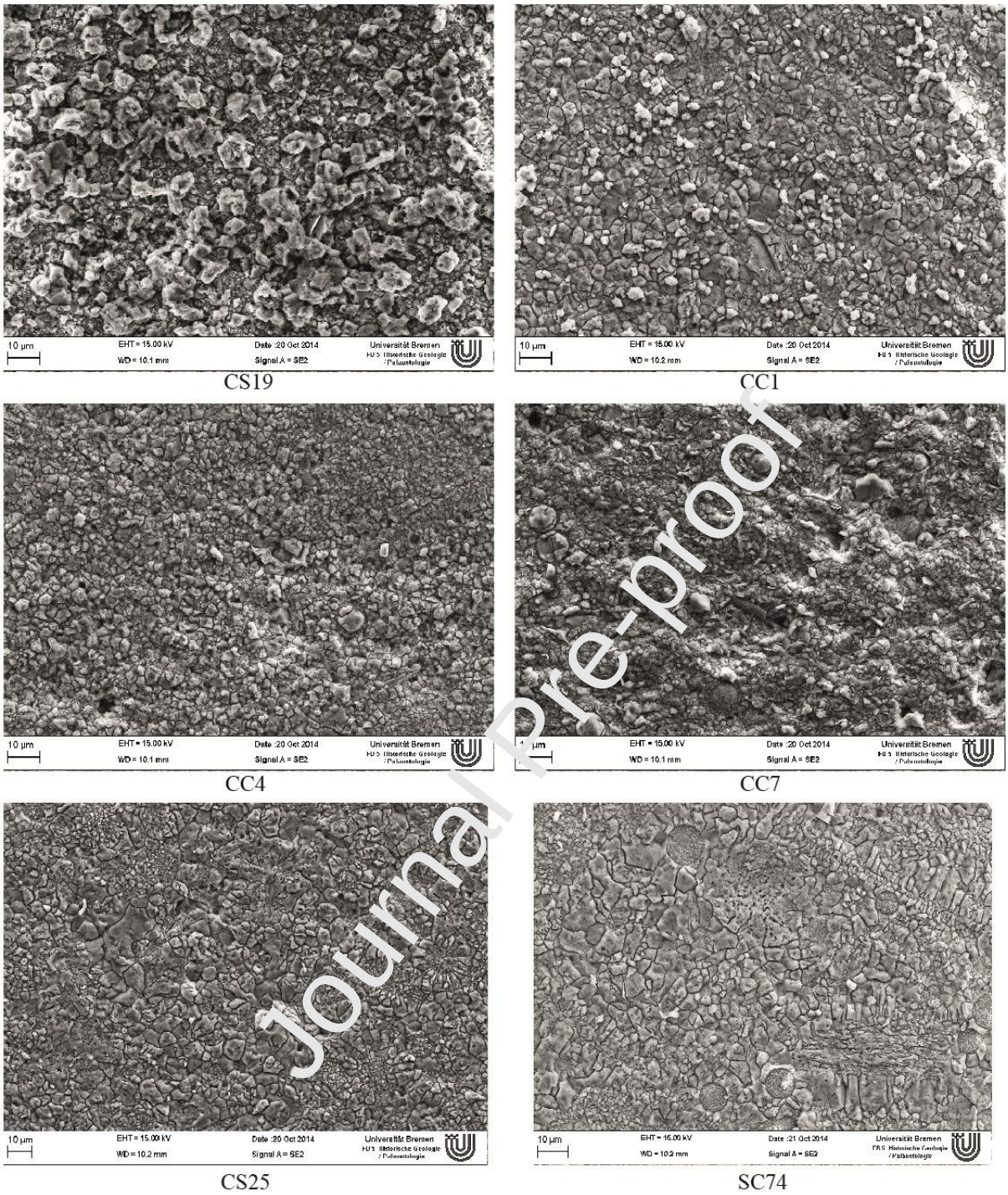

Figure A1. FESEM images of selected samples from the Transdanubian Range (CC and CS) and the Western Julian Alps (SC).

Highlights

- Calcispheres were studied in successions across the Carnian Pluvial Episode (CPE)
- In Western Tethys Calcispheres are abundant from the onset of the CPE
- They belong to the genus *Orthopithonella*
- They were a significant component of CPE hemipelagic–pelagic limestones